Journal of Materials Science Research and Reviews

1(3): 1-14, 2018; Article no.JMSRR.43380

Analysis of Electronic Structure and X-ray Absorption and Emission Spectra in MgO within the FP-LAPW Method

G. B. Grad[1*], E. R. González[1], J. Torres Díaz[1] and E. V. Bonzi[1]

[1] *FaMAF, Universidad Nacional de Córdoba, Medina Allende s/n (5010), Córdoba, Argentina.*

Authors' contributions

This work was carried out in collaboration between all authors. Author GBG designed the study and performed the calculations. Author ERG managed the literature searches. Authors JTD and EVB analysed the results and performed the graphics. Authors GBG and EVB wrote the manuscript. All authors read and approved the final manuscript.

Article Information

DOI: 10.9734/JMSRR/2018/43380

Editor(s):

(1) Dr. Madogni Vianou Irenee, Departement de Physique, Laboratoire de Physique du Rayonnement LPR, Cotonou, Universite dAbomey-Calavi (UAC), Benin.

(2) Dr. Moumi Pandit, Associate Professor, Department of Electrical & Electronics Engineering, Sikkim Manipal Institute of Technology, Sikkim Manipal University, India.

Reviewers:

(1) Konrad Gruszka, Czestochowa University of Technology, Poland.

(2) Yakoubi Abdelkader, University Djillali Liabes of Sidi-Bel-Abbes, Algeria.

(3) Adolfo Quiroz Rodriguez, Universidad Autónoma del Carmen, Mexico.

Complete Peer review History: http://sciencedomain.org/review-history/26508

Received: 17 July 2018

Accepted: 26 September 2018

Published: 05 October 2018

Original Research Article

Abstract

In this work we calculated MgO *ab initio* X-ray Absorption and Emission spectra using the Full Potential Linearized Augmented Plane Wave method within the Density Functional Theory formalism. The X-ray Absorption and Emission spectra for the K and $L_{2,3}$ edges of Mg and O atoms were calculated including a core hole in order to study the electronic structure of valence and conduction bands of the system. Both kinds of spectra were compared with experimental data obtaining a very good agreement and the improvement in the spectra due to the use of Tran Blaha modified Becke-Johnson (TB-mBJ)potential is manifested. This potential describes better the insulator properties, produces a band gap that is in good agreement with the experimental value and improves the intensities and the structure of the spectra. Was interesting to find the presence of Mg d states below the Fermi energy in the equilibrium volume of MgO.

**Corresponding author: E-mail: grad@famaf.unc.edu.ar*

The XANES experiments were better reproduced by introducing the full core hole in the calculations using TB-mBJ potential while for XES the best agreement was obtained without core hole.
The Bader's topological method was employed to analyse the ionic behaviour. Using the electronic charges obtained with the Bader's Method and the equilibrium lattice parameter, we obtained the value of the Lattice Energy and we compared it with the value obtained by the Born-Haber cycle showing a good agreement. The charge density for MgO was plotted, and a maximally localized Wannier function for O is shown.

Keywords: Core hole; K and L 2,3 edges; ab-initio calculations; XANES; XES.

2018 53C25; 83C05; 57N16.

1 Introduction

X-ray Absorption Near Edge and Emission Spectroscopy (XANES and XES) involve the interaction of X-ray with matter and are among the most important tools for the characterization of the electronic structure of the materials through the analysis of the densities of states, the valence and conduction bands and of the optical properties. The XANES technique involves the absorption of photons to excite electrons from deep core levels, such as a $1s$ electron of a selected atom, to an unoccupied state, leaving behind a core hole. The XES technique consists in the filling of a core hole by a valence electron causing the emission of an X-ray photon. XANES gives information of the excited states and XES gives information of the chemical bonding, by combining XANES and XES, one can obtain information about the electronic structure of unoccupied states (conduction band) and occupied states (valence band). Several experimental [1, 2] and theoretical calculations using different approaches [3, 4] carried out XANES and XES studies.

Within the Independent Particle Approximation (IPA), the XANES is proportional to the unoccupied part of the projected electronic Density Of States (DOS) weighted by the transition probability under the dipolar approximation from the core to the conduction states, the XES spectra is proportional to the occupied part of the projected DOS. These spectra are usually calculated by means of *ab initio* methods [5, 6].

In the *ab initio* methods the local-density approximation (LDA) [7] or the generalized gradient approximation (GGA) [8] usually are good choices, but fail when calculating semiconductor and insulator densities of states. A modified Becke-Johnson exchange potential was tested by Tran and Blaha for the calculation of band gaps giving much better results [9, 10] for such semiconductors and insulator materials.

In this work we performed all-electron calculations within the Density Functional Theory (DFT) formalism [11, 12] with different potentials: Perdew-Burke-Ernzerhof (PBE) [8], Generalized Gradient Approximation plus Hubbard U parameter [13] and Tran Blaha modified Becke-Johnson (TB-mBJ) [14] to study the X-ray K and L MgO spectra.

The results of calculated X-ray near edge absorption spectra from core level $1s$ and $2p$ states to the conduction band, were compared against the experimental K and L spectra, from this comparisons we choose the potential that produces the best agreement. We considered X-ray emission transitions from the valence band to the $1s$ (K spectrum) and $2p$ (L spectrum) levels of the Mg atom and to the $1s$ (K spectrum) level of the O atom.

It is an important question how a vacancy formed at a core level of the Mg atom affects the electronic structure and spectrum of the crystal. There are two possible limiting cases, namely, either the vacancy charge is completely screened, and the vacancy does not affect the spectrum, or the vacancy charge is not screened at all and is equal to unity. In the latter case, the vacancy can be considered as a point defect. The hole left by the excited core electron affects the electronic structure of the crystal, to

consider this effect we performed XANES and XES spectra introducing partial core holes within the Slater [15, 16] approximation, using supercell calculations.

We analysed the partial contributions of the densities of states (DOS) calculated using these potentials in comparison with the broadened and the unbroadened K and L edges of MgO. The hole left by the excited core electron changes the electronic structure of the crystal, however the effect of this core hole is not always observable. The XANES experiments were better reproduced by introducing the full core hole in the calculations using TB-mBJ potential while for XES the best agreement was obtained without core hole.

2 Theoretical Method

The *ab initio* calculations were carried out using the WIEN2k 16 package [17, 18, 19], which uses all electron self-consistent calculations based on the scalar relativistic full-potential linearized augmented plane-wave basis set combined with local orbitals (FP-LAPW+lo). This is one of the most accurate schemes to solve the Kohn-Sham equations of Density Functional Theory [11, 12].

It has been shown [11] that the ground-state energy of an interacting inhomogeneous electron gas in a potential $v(\mathbf{r})$ can be written:

$$E = \int v(\mathbf{r})n(\mathbf{r})d\mathbf{r} + \frac{1}{2}\int\int \frac{n(\mathbf{r})n(\mathbf{r}')}{|\mathbf{r}-\mathbf{r}'|}d\mathbf{r}d\mathbf{r}' + G[n] \tag{2.1}$$

$$G[n] \equiv T_s[n] + E_{xc}[n] \tag{2.2}$$

$$E_{xc}[n] = \int n(\mathbf{r})\epsilon_{xc}(n(\mathbf{r}))d\mathbf{r} \tag{2.3}$$

where $n(\mathbf{r})$ is the density of an electron uniform gas, $G[n]$ is a universal functional of the density, the T_s is the kinetic energy of a system of non-interacting electrons, $E_{xc}[n]$ is the exchange and correlation energy of an interacting system and ϵ_{xc} is the exchange and correlation energy per electron of a uniform gas of density $n(\mathbf{r})$.

For a given potential $n(\mathbf{r})$ is obtained solving the one-particle Kohn-Sham (K-S) Schrödinger equations [12]:

$$\left\{-\frac{1}{2}\nabla^2 + [\varphi(\mathbf{r}) + \mu_{xc}(n(\mathbf{r}))]\right\}\psi_i(\mathbf{r}) = \epsilon_i\psi_i(\mathbf{r}) \tag{2.4}$$

setting

$$n(\mathbf{r}) = \sum_{i=1}^{N}|\psi_i(\mathbf{r})|^2 \tag{2.5}$$

where N is the number of electrons and the $\mu_{xc}(n(\mathbf{r}))$ is the exchange and correlation contribution to the chemical potential.

The LDA and GGA functionals usually yield ground-state properties, which are in reasonable agreement with the experiments. However, this sometimes is not the case for excited-state properties.

Methods that retain the computational efficiency of standard DFT but improve the spectroscopic properties are potentially of great interest, consequently improvement has been achieved by LDA+U [13] and a modified version (TB-mBJ) [10, 14, 20] of the Becke and Johnson (BJ) exchange potential [9], who proposed $v(r)$ to reproduce the exact exchange potential in atoms:

$$v_x^{BJ}(\mathbf{r}) = v_x^{BR}(\mathbf{r}) + \frac{1}{\pi}\sqrt{\frac{5}{12}}\sqrt{\frac{2t(\mathbf{r})}{\rho(\mathbf{r})}} \tag{2.6}$$

where $\rho = \sum_{i=1}^{N}|\psi_i|^2$ is the electron density,

$$t(\mathbf{r}) = \frac{1}{2}\sum_{i=1}^{N}\nabla\psi_i^*(\mathbf{r})\cdot\nabla\psi_i(\mathbf{r}) \tag{2.7}$$

is the K-S kinetic-energy density, and

$$v_x^{BR}(\mathbf{r}) = -\frac{1}{b(\mathbf{r})}\left(1 - e^{-x(\mathbf{r})} - \frac{1}{2}x(\mathbf{r})e^{-x(\mathbf{r})}\right) \tag{2.8}$$

BJ potential leads to only moderately improved band-gaps, a simple modification of BJ potential was propose by Tran and Blaha [14]

$$v_x^{TB-mBJ}(\mathbf{r}) = cv_x^{BR}(\mathbf{r}) + (3c-2)\frac{1}{\pi}\sqrt{\frac{5}{12}}\sqrt{\frac{2t(\mathbf{r})}{\rho(\mathbf{r})}} \tag{2.9}$$

where c is a parameter obtained according to a fit to the experimental band-gaps.

The TB-mBJ calculations are produced after

the PBE or LDA convergence is achieved self consistently, they are used as a starting point for TB-mBJ.

We can calculate near edge structure of X-ray absorption and emission spectra according to the formalism described by Schwarz et al. [5, 6] for the dipole allowed transitions.

$$I_K(E) \propto \frac{1}{3} E^3 M^2(p, 1s, \epsilon) \varkappa_p(\epsilon) \tag{2.10}$$

$$I_{L_{III}}(E) \propto E^3 \left(M^2(s, 2p, \epsilon) \varkappa_s(\epsilon) + \frac{2}{5} M^2(d, 2p, \epsilon) \varkappa_d(\epsilon) \right) \tag{2.11}$$

In these equations, $E = \epsilon - \epsilon_{core}$, denotes the energy of the emitted X-rays, $\varkappa_l(\epsilon)$ are the local partial (l-like) densities of valence states corresponding to energy ϵ of the valance electron and $M^2(l, n'l', \epsilon)$ are the radial transition probabilities from l-like valence state of energy ϵ to a core hole characterised by the quantum numbers $n'l'$ and energy ϵ_{core}.

Slater's transition state method enables us to calculate excitation energies, considering the removal of half an electron of the state of study [15, 16], to calculate excitation energies. So we use fractional core holes to find the optimal match with the experiments.

The calculations were produced without core hole and with core holes of 0.5 and 1.0 and the one that shows the best agreement with the experiment was compared with the partial densities of states that contributes to the edge.

The XANES and XES spectra were calculated for K and L lines and they were convoluted with a Lorentzian to account for lifetime broadening and resolution of the spectrometer. The required precision in total energy was achieved by using a large plane-wave cut-off of $RK_{\text{max}} = 8$, (where R is the muffin-tin radius and K_{max} is the cut-off in the plane wave expansion of wave functional), resulting in a kpoint sampling in the Brillouin zone (BZ) of 500 points. Muffin-tin radius had to be increased in Mg atom, to have the p electrons in the atom core to calculate Mg $L_{2,3}$ edges. Rmt(Mg) = 2.45 a.u. and Rmt(O)= 1.45 a.u.. The analysis was carried out at the theoretical equilibrium volume based on PBE and GGA+U calculations.

3 The supercells

The artificial core hole interactions created by the periodic boundary conditions can be reduced by enlarging the distances between the core holes, usually, the Slater's method requires the use of supercells in order to do this, then supercell and single cell calculations were used to analyse the hole-hole effect. We optimized the MgO cubic structure, rocksalt family, with space group Fm-3m, in order to obtain the lattice parameter. We experimented with supercells of different sizes for the MgO structure and the calculations were performed employing a 2x2x2 supercell of 64 atoms.

4 Results and discussion

In this work we performed *ab initio* calculations in order to analyse the electronic properties, DOS, XANES and XES spectra for the different edges of MgO. The MgO cubic structure was optimized and the lattice parameter obtained self-consistently using PBE calculations was 4.261 Å, and using GGA+U was 4.259 Å, which are slightly larger than the experimental MgO lattice parameter 4.186 Å. The GGA+U calculations give a slightly better lattice parameter than the PBE compared to the experiments. The PBE result is exactly the same as the one obtained by Haas *et al.* [21] where a very thorough comparison of the lattice parameters using different functionals are produced.

The band gap is also calculated using different potentials and compared to the experimental value. The band gap obtained with the PBE calculation is 4.42 eV, the band gap obtained with GGA+U is 4.43 eV for three different U values, (3.5 eV, 5 eV and 7 eV) which are similar to values obtained in the literature with those potentials [22], the difference was produced by the TB-mBJ calculation giving 7.16 eV which compares much better than the others with the experimental one 7.83 eV [10], showing MgO is an insulator. The direct band gap in Γ-point is shown in the band structure plot in Fig. 1.

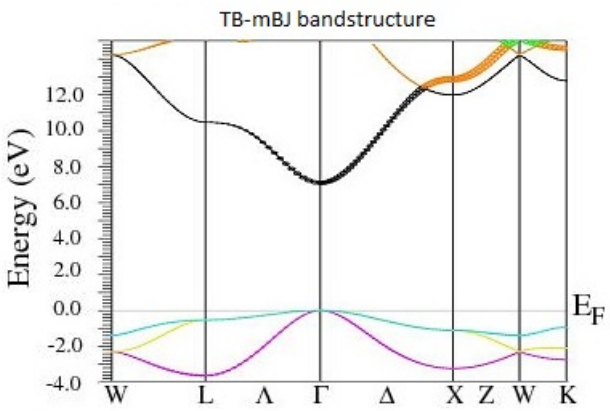

Fig. 1. The MgO bandstructure is shown with the increased pick for the s states of Mg atoms. The direct band gap for the Γ point is of 7.16 eV

4.1 X-ray Absorption Spectroscopy

We considered transitions from the $1s$ (K edge) and $2p$ ($L_{2,3}$ edge) core levels of Mg atom and from the $1s$ (K edge) core level of O atom to the conduction band. We calculated PBE and TB-mBJ XANES spectra including the fractional core hole technique and compared to the experimental data [1, 2] to obtain the best match, which was obtained with the full core hole.

In Figs. 2 and 3 we show the calculated Mg $L_{2,3}$ spectra using PBE and TB-mBJ with full core hole compared with the experimental spectrum obtained by OBrien *et al.* [2]. The first peak in the XANES experimental spectrum just above the energy gap, around 8 eV corresponding to the s states is smaller using PBE than TB-mBJ. The intensity relationship of the s states with respect to the d states is better described by the TB-mBJ calculation. For the higher energies, the spectrum using TB-mBJ shows better agreement with the experimental spectrum as well. The higher energy region of the spectrum is mainly produced by d states, the positions of the peaks using TB-mBJ show better agreement with the experiment than the PBE calculation.

In Figs. 4 and 5 we show the O K and Mg K spectra calculated using TB-mBJ and full core hole, compared to the corresponding experimental spectra produced by Luches *et al.* [1] and the corresponding p DOS states of both atoms. We show TB-mBJ calculations as they have better agreement with the experimental spectra [1, 2] compared to PBE calculations.

The peaks of the calculated Mg K spectrum corresponding to the p states, shown at the bottom of Fig. 5, are in the correct positions and the intensities compare very well with the experimental ones.

In the O K spectrum, the position of the p states is correct, the intensities, in general, compare very well with the experimental spectrum, except for the lower energies where there is a slight difference.

We observed, as was described for other systems [23], that the MgO XANES spectra using the TB-mBJ potential and a full core hole shows the best agreement with the experiments and provide a better description of the excited states.

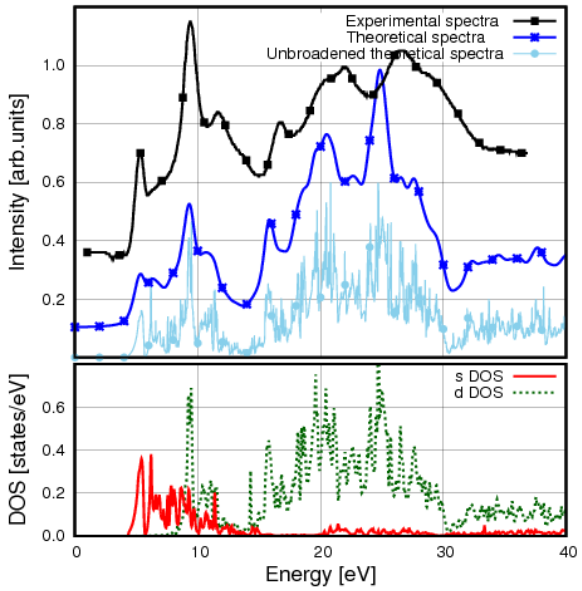

Fig. 2. Broadened and unbroadened Mg XANES $L_{2,3}$ edges spectrum calculated using PBE with full core hole compared to the s, d-projected DOS. The experimental spectrum shown was measured by OBrien et al. [2]

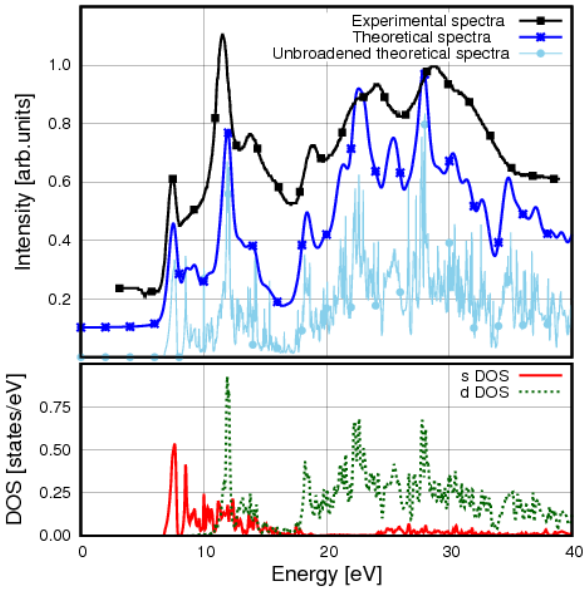

Fig. 3. Broadened and unbroadened Mg XANES $L_{2,3}$ edges spectrum calculated using TB-mBJ potential with full core hole compared to the s, d-projected DOS. The experimental spectrum shown was measured by OBrien et al. [2]

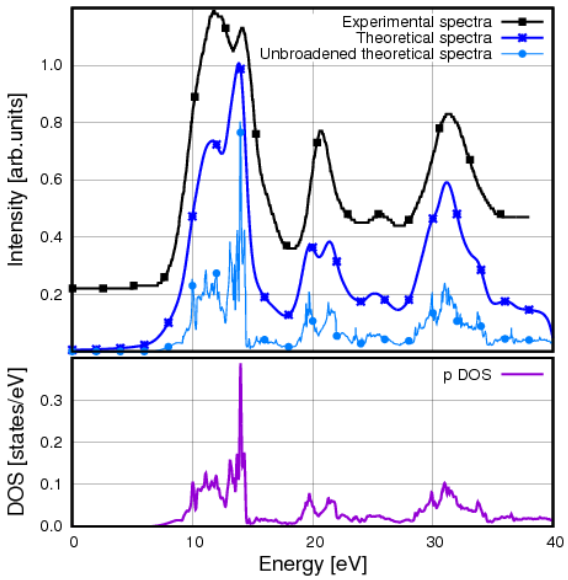

Fig. 4. Broadened and unbroadened O XANES K edge spectrum calculated using TB-mBJ potential with full core hole compared to the p-projected DOS. The experimental spectrum shown was measured by Luches et al. [1]

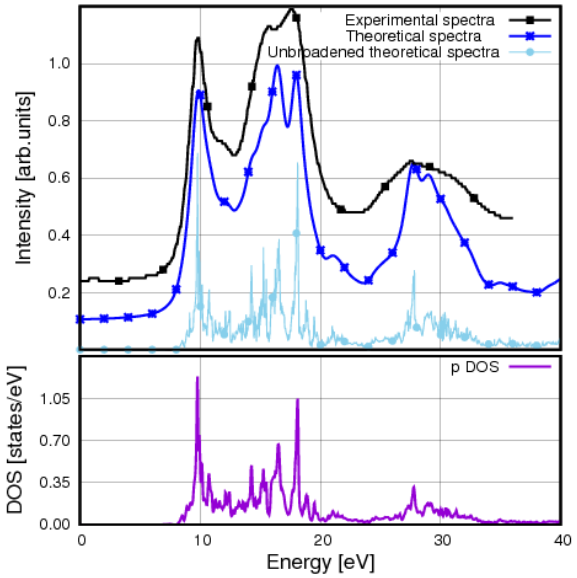

Fig. 5. Broadened and unbroadened Mg XANES K edge spectrum calculated using TB-mBJ potential with full core hole compared to the p-projected DOS. The experimental spectrum shown was measured by Luches et al. [1]

4.2 X-ray Emission Spectroscopy

We also analysed XES transitions from the valence band to the $1s$ (K edge) and $2p$ ($L_{2,3}$ edge) levels for Mg atom and from the valence band to the $1s$ (K edge) for O atom.

In Figs. 6 and 7 we show the O K and Mg K calculated spectra using TB-mBJ compared to the experiments produced by Galakhov et al. [24] and Jonnard et al. [25] respectively and the corresponding p-projected DOS states. The Mg $L_{2,3}$ spectrum using TB-mBJ is shown in Fig. 8 compared with the experimental spectrum shown by Ovcharenko et al. [26, 27, 28, 29, 30] and the corresponding s and d-projected DOS states.

The valence DOS contributions are mainly from O $2p$ states hybridized with Mg $3s$ and $3p$ states. The best agreement with the experiment is obtained without core hole in PBE and TB-mBJ, this makes sense as the XES final state has no core hole.

In the unbroadened Mg $L_{2,3}$ spectrum the s contribution is bigger than the d contribution, the same trend is observed in the DOS plot. The broadened spectrum inverts the relationship between these peaks in agreement with the experiment in both, PBE and TB-mBJ calculated spectra.

There is a small d contribution in the density of states below the Fermi energy identified as well in the XES Mg $L_{2,3}$ spectrum, on the contrary in reference [28] the authors deny this presence. However, it is expected that the packing in MgO makes d bands move down in energy, so the number of d states below the Fermi energy increases respect to the Mg free atom. In MgO the d states effect becomes more important due to the proximity with the oxygen, than in metallic Mg, where the d contributions are almost negligible in the valence band compared to the s and p contributions.

To show this effect is more important when the volume of the cell decreases and the oxygen atom becomes closer to the magnesium atom, we performed calculations for different volumes of the unit cell showing the evolution of d-projected states from bigger values to the equilibrium value of the unit cell. In Fig. 9 the d states contribution is almost negligible for 100 percent bigger unit cell and starts to increase when it is smaller.

Moreover, the shift in energy of the d states to lower energies is observed when the volume of the cell decreases to the equilibrium value.

In the experimental Mg XES $L_{2,3}$ spectrum there is an extra peak which is not observed in the calculated spectrum. We calculated the transitions corresponding to the Mg $L_{2,3}$ contributions and we include the intrashell $2p \rightarrow 2s$ transition as well, shown in Fig. 10.

Our plot was produced with the numerical convolution between $3s$ and $3d$ states with $2p$ states, the same procedure was applied to the $2p \rightarrow 2s$ transition, as these are states that belong to the same $n = 2$ level we call them intra-shell transitions. This extra transition corresponds to the same energy as the extra experimental peak observed. This scheme was performed assuming a plain transition matrix, so the intensity should not be considered. It could have been produced in the experiment by an unwanted excitation of the $2s$ level and filled again by a transition $2p \rightarrow 2s$, present in a very small proportion.

Our X-ray Mg $L_{2,3}$ emission spectrum agrees better with the XPS shown by King *et al.* [28] than with the experiment in references [26, 27] because XPS does not get the extra peak, this confirms it does not belong to the Mg $L_{2,3}$ edge, and should be an artefact of the measurement.

4.3 Charge density

In order to analyse the chemical bonding, we study the valence-charge density. The (110) plane of the MgO charge density is plotted in Fig. 11(a), Mg atoms (at the centre and at the corners) have very little charge, while the O atoms concentrate most of the electronic charge density. As expected in ionic solids, the electrons are transferred from the electro-positive atom to the electro-negative atom.

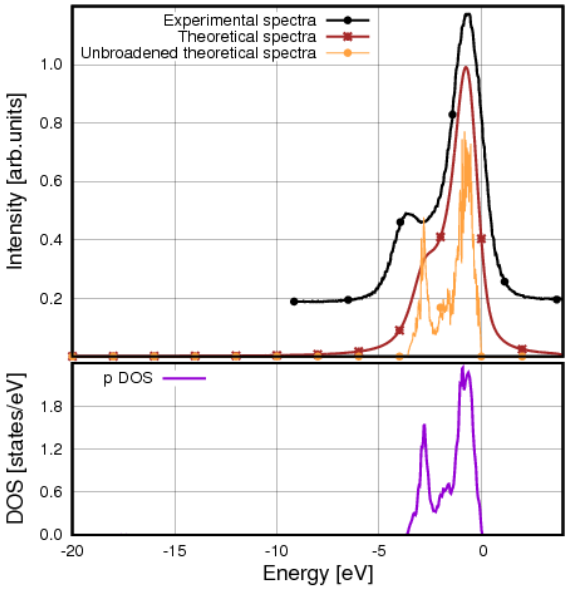

Fig. 6. Broadened and unbroadened O K XES spectrum calculated using TB-mBJ potential without core hole in MgO compared to p-projected DOS. The experimental spectrum shown was measured by Galakhov et al. [24]

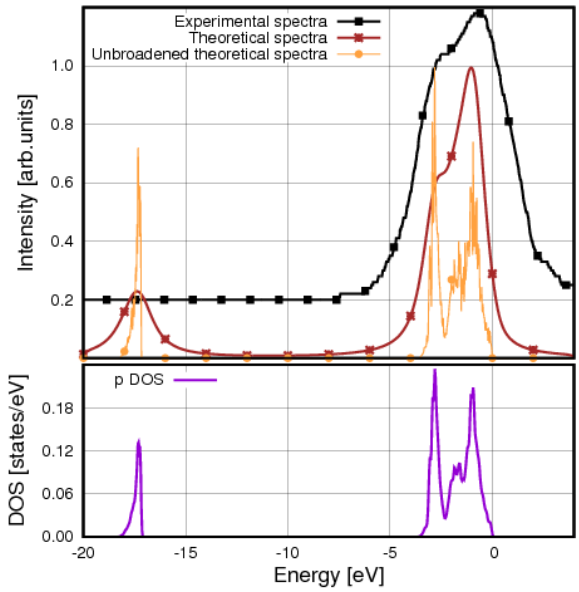

Fig. 7. Broadened and unbroadened Mg K XES spectrum compared to s and d-projected DOS calculated using TB-mBJ potential without core hole in MgO. The experimental spectrum was obtained from Milov et al. [27]

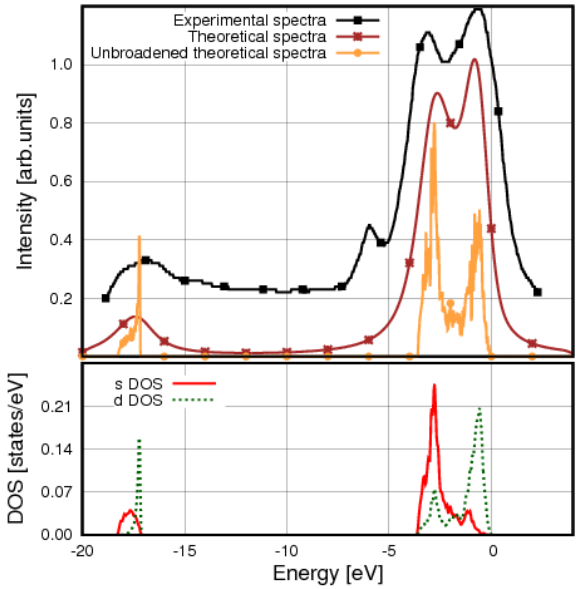

Fig. 8. Broadened and unbroadened Mg $L_{2,3}$ XES spectrum compared to s and d-projected DOS calculated using TB-mBJ potential without core hole in MgO. The experimental spectrum was obtained from Ovcharenko et al. [26]

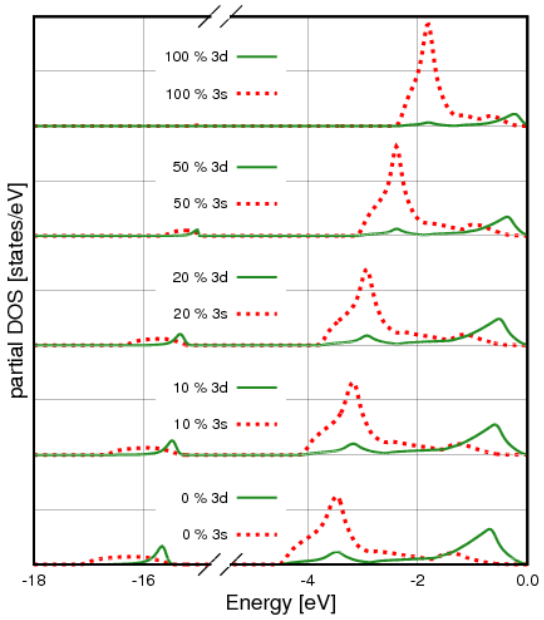

Fig. 9. s and d projected DOS contributions as a function of the volume

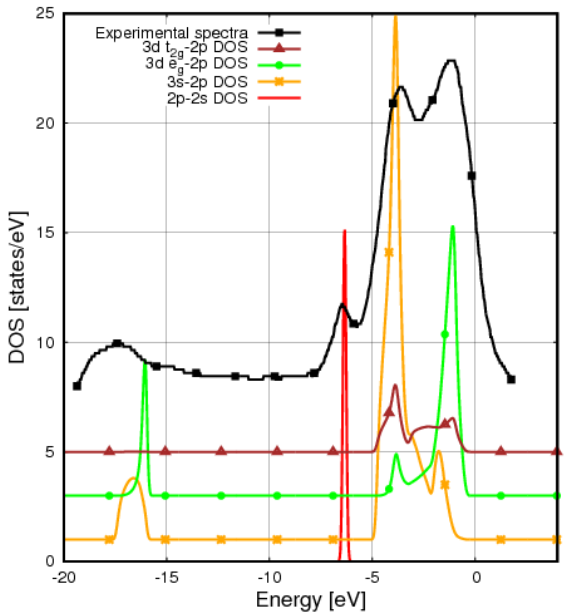

Fig. 10. XES Mg $L_{2,3}$ scheme plus 2$p \rightarrow$ 2s extra peak

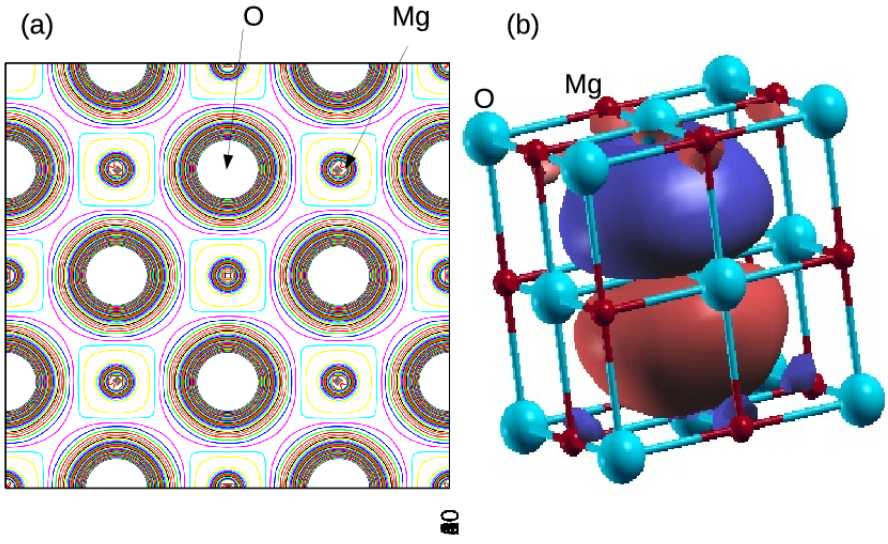

Fig. 11. Electronic charge density plot on the (110) plane (a) and the oxygen Wannier function (b)

The wannierization procedure was implemented selecting a group of Bloch bands for which the maximally localized Wannier functions (MLWF) were calculated using Wannier90 according to the Marzari and Vanderbilt method [31] and Mostofi et al. [32]. The Wannier functions form an orthogonal and complete basis set to express the Hamiltonian. The energy range selected corresponds to the valence band, as these bands do not overlap in energy with others the disentanglement procedure was not necessary. The Bloch states are projected over the atomic like p and s orbitals centred around O and Mg atoms. After an iterative procedure, the MLWF were determined and the calculation shows the charge density is in the neighbourhood of the O atom. The symmetry is similar to the real spherical harmonics with $l = 1$ as shown in Fig. 11(b) for one isovalue of O atom. The MLWF are not strictly identical to the atomic orbitals, the tails (not shown here) have different symmetry as it is also expected.

Baders method, explained in the book Atoms in Molecules [33], was developed by J. Fuhr in his program AIM (Atoms in Molecules). We applied this method to analyse the topology of the charge density to determine the total charge of Mg and O atoms and the charge transfer from Mg to O.

After the selfconsistent calculation, AIM provides the volume that belongs to each atom and integrates the charge in that volume. Mg volume is 31.279 a.u. and the total electronic charge is 10.276 electrons, which indicates a loss of charge equivalent to 1.724 electrons, compared to the free Mg atom. O volume is 99.159 a.u. and the total electronic charge is 9.724 electrons, which indicates a gain of charge equivalent to 1.724 electrons, compared to the free O atom, meaning Mg transferred the charge of almost two electrons to the O atom, which is consistent with the expected trends in ionic solids.

Using the electronic charges obtained with the Bader's topological Method, the Coulomb potential and the Madelung constant of 1.74756, we obtained the value of Lattice Energy equal to 3377 kJ/mol using the equilibrium lattice parameter and equal to 3429 kJ/mol when the experimental lattice parameter was used; we compared them with the 3890 kJ/mol value obtained by the Born-Haber cycle.

The equations used for the electrical potential and the lattice energy [34] were:

$$V = \frac{1}{4\pi\epsilon_0}\frac{Q^2}{\left(\frac{a}{2}\right)}$$

$$LatticeEnergy = V.\chi.Av$$

The values used were

$\epsilon_0 = 8.8541878176.10^{-12}\frac{C^2}{Nm^2}$

$Q = 2.762.10^{-19}[C]$, it is the charge value $1.724[e]$ expressed in C

$a = 4.261.10^{-10}[A]$, the lattice parameter value is divided by two, because we need the distance from Mg to O.

$Av = 6.022140857.10^{23}$ the Avogadro number.

$\chi = 1.747564594633182$ the Madelung number for MgO.

Since we used the transferred charge, then the Born exponent factor should not be included. The value we obtained is smaller than the Born-Haber cycle, we believe that it is because, in the calculation of the Coulomb potential, we considered the charge concentrated in one point of the space and not as a spatial distribution. The O distribution of charge is more extended than Mg distribution according to Bader, this is consistent with the charge density plot in Fig. 11(a) where the O atom concentrates most of the electronic charge and the p character of the O orbital are shown in Fig. 11(b) by the oxygen MLWF function.

5 CONCLUSIONS

In this work MgO X-ray Absorption Near-Edge and X-ray Emission Spectra spectra were calculated using different potentials Perdew-Burke-Ernzerhof (PBE) [8], Generalized Gradient Approxi-mation plus Hubbard U parameter (GGA+U) [13] and Tran Blaha modified Becke-Johnson (TB-mBJ) [10, 14, 20] and compared with experimental results [1, 2, 24, 26, 27, 28].

The experiments were better reproduced by introducing the full core hole in the calculations using TB-mBJ potential. Furthermore, our X-ray Mg $L_{2,3}$ absorption spectra calculated

using TB-mBJ potential and full core hole compares better with the experiment than the one calculated by Olovsson *et. al.* [4] using the BSE formulation. The BSE theory, though it is a better approximation is not needed in this case. The TB-mBJ is worth using as this functional describes better the semiconductors and insulators, produces band gaps that are in very good agreement with the experimental values and improves the structure of the spectra.

The DFT is formally a theory for the ground state, nevertheless, it gives a good estimate in properties that involve excited energy states like absorption or emission spectra [6].

Our XES calculations were compared with experimental results for Mg K and $L_{2,3}$ XES spectra [27, 29, 30] and O K [24]. The best agreement was obtained without core hole. The calculated XES spectra reproduce the main features of the experimental spectra for the Mg K, O K and Mg $L_{2,3}$edges.

There is a small experimental peak not reproduced by the calculated Mg $L_{2,3}$ XES spectrum because this only reflects the transition from valence states to 2p states. This peak could have been produced by an undesired excitation of the 2s states. We consider that finding these intrashell transitions in Mg atom is relevant, as is normally expected in bigger atoms like uranium.

The intensities relationship of the $3s$ and $3d$ contributions in Mg $L_{2,3}$ spectrum is improved respect to the PBE potential and the low energy peaks are better reproduced. In the experimental spectrum the s contribution is smaller than d, the same behaviour is shown using the proper broadening parameter in both PBE and TB-mBJ calculated spectra. This behaviour shows that the TB-mBJ potential not only corrects the band gap but also improves the intensities of the peaks as well. We show the presence of Mg d states below the Fermi energy in the equilibrium volume of MgO.

We obtained the total charge of Mg and O atoms in the MgO equilibrium unit cell after the self consistent calculation is converged, this shows that a very important part of the $3s$ electronic charge of the Mg atoms has been transferred to the O atom in agreement with the ionic behaviour of MgO. Our value of the Lattice Energy is comparable in order of magnitude with the empirical Born-Haber cycle value.

ACKNOWLEDGEMENT

This work was supported with grants provided by SeCyT U.N.C. (Argentina). This work used Mendieta Cluster from CCAD-UNC, which is part of SNCAD-MinCyT, Argentina. We would also like to thank Dr. Rainer Schweinfest and Dr. Raúl T. Mainardi for their help and valuable discussions and Dr. Javier Fuhr for his program AIM based on the Bader's Method.

COMPETING INTERESTS

Authors have declared that no competing interests exist.

References

[1] Luches P, D'Addato S, Valeri S, Groppo E, Prestipino C, Lamberti C, Boscherini F. Phys. Rev. B 2004;69:045412.

[2] OBrien W, Jia J, Dong Q, Callcott T, Rubensson J, Mueller D, Ederer D. Phys. Rev. B 1991;44:1013.

[3] Laskowski R, Blaha P. Phys. Rev. B. 2010;82:205104.

[4] Olovsson W, Tanaka I, Mizoguchi T, Puschnig P, Ambrosch-Draxl C. Phys. Rev. B. 2009;79:041102.

[5] Schwarz K, Neckel A, Nordgren J. J Phys. F. Metal Phys. 1979;9:2509.

[6] Schwarz K, Wimmer E. J. Phys. F. Metal Phys. 1980;10:1001.

[7] Perdew JP, Wang Y. Phys. Rev. B. 1992;45:13244.

[8] Perdew JP, Burke K, Ernzerhof M. Phys. Rev. Lett. 1996;77:3865.

[9] Becke AD, Johnson ER. J Chem. Physics. 2006;124:221101.

[10] Tran F, Blaha P. Phys. Rev. Lett. 2009;102:226401.

[11] Hohenberg P, Kohn W. Phys. Rev. 1964;136:B864.

[12] Kohn W, Sham LJ. Phys. Rev. 1965;140:1133.

[13] Anisimov V, Gunnarsson O. Phys. Rev. B. 1991;43:7570.

[14] Koller D, Tran F, Blaha P. Phys. Rev. B. 2012;85:155109.

[15] Slater JC, Johnson KH. Phys. Rev. B. 1972;5:844.

[16] Liberman DA. Phys. Rev. B. 2000;62:6851.

[17] Madsen GKH, Blaha P, Schwarz K, Sjostedt E, Nordström L. Phys. Rev. B. 2001;64:195134.

[18] Blaha P, Schwarz K, Madsen GKH, Kvasnicka D, Luitz J. WIEN2k: An Augmented Plane Wave + Local Orbitals Program for Calculating Crystal Properties. (Karlheinz Schwarz, Techn. Universität Wien, Austria); 2001. ISBN 3-9501031-1-2.

[19] Schwarz K, Blaha P, Madsen GKH. Computer physics communications. 2002;147:71.

[20] Tran F, Blaha P, Schwarz K. J. Phys.: Condens. Matter. 2007;19:196208.

[21] Haas P, Tran F, Blaha P. Phys. Rev. B. 2009;79:085104.

[22] Baltache H, Khenata R, Sahnoun M, Driz M, Abbar B, Bouhafs B. Physica B. 2004;344.

[23] Hetaba W, Blaha P, Tran F, Schattschneider P. Phys. Rev. B. 2012;85:205108.

[24] Galakhov V, Finkelstein L, Zatsepin D, et al. Phys. Rev. B. 2000;62(8):4922.

[25] Jonnard P, Vergand F, Bonnelle C, Orgaz E, Gupta M. Phys. Rev. B. 1998;57:12111.

[26] Ovcharenko R, Tupitsyn I, Kuznetsov V, Shulakov A. Optics and Spectroscopy. 2011;111:940.

[27] Milov I, Abarenkov I, Tupitsyn I. Optics and Spectroscopy. 2015;118:519.

[28] King P, Veal TD, Schleife A, et al. Phys. Rev. B. 2009;79:205205.

[29] Hanson W, Arakawa E, Williams M. Journal of Applied Physics. 1972;43:1661.

[30] Fischer DW, Baun WL. Spectrochimica Acta. 1965;21:443.

[31] Marzari N, Vanderbilt D. Phys. Rev. B. 1997;56:12847.

[32] Mostofi AA, Yates JR, Pizzi G, et al. Computer Physics Communications. 2014;185:2309.

[33] Bader R, co-workers. AIMPAC: A Suite of Programs for the Theory of Atoms in Molecules: A Quantum Theory, Hamilton, Canada. Clarendon Press, Oxford; 1990. (Available: http://www.chemistry.mcmaster.ca/aimpac)

[34] Barry Carter C, Grant Norton M. Ceramic Materials - Science and Engineering-Springer (2007) ISBN: 0387462708.

Peer-review history:
The peer review history for this paper can be accessed here (Please copy paste the total link in your browser address bar)
http://sciencedomain.org/review-history/26508